


Magnetic field induced transition from a vortex liquid to Bose metal in ultrathin *a*-MoGe thin filmSurajit Dutta, John Jesudasan , and Pratap Raychaudhuri **Tata Institute of Fundamental Research, Homi Bhabha Road, Mumbai 400005, India* (Received 21 November 2021; revised 2 February 2022; accepted 21 March 2022; published 7 April 2022; corrected 26 July 2022)

We find transport and spectroscopic signatures that are consistent with a magnetic field induced transition from a vortex liquid to Bose metal in a two-dimensional amorphous superconductor, *a*-MoGe, using a combination of magnetotransport and scanning tunneling spectroscopy (STS). Below the superconducting transition, $T_c \sim 1.36$ K, the magnetoresistance isotherms cross at a nearly temperature independent magnetic field, $H_c^* \sim 36$ kOe. Above this field, the temperature coefficient of resistance is weakly negative, but the resistance remains finite as $T \rightarrow 0$, as expected in a bad metal. From STS conductance maps and transport measurements at 450 mK we observe a very disordered vortex lattice at very low fields that melts into a vortex liquid above 3 kOe. Up to H_c^* the tunneling spectra display a superconducting gap and coherence peak over a broad background caused by electron-electron interactions, as expected in a vortex liquid. However, above H_c^* the tunneling spectra continue to display the gap but the coherence peak gets completely suppressed, suggesting that Cooper pairs lose their phase coherence. We conclude that H_c^* demarcates a transition from a vortex liquid to Bose metal, that eventually transforms to a regular metal at a higher field H^* where the gap vanishes in the electronic spectrum.

DOI: [10.1103/PhysRevB.105.L140503](https://doi.org/10.1103/PhysRevB.105.L140503)**I. INTRODUCTION**

The survival of Cooper pairing even after the global phase coherence is destroyed has been a recurring theme in strongly disordered and two-dimensional superconductors [1–4]. In zero field, the zero resistance state can get destroyed due to phase fluctuations at the superconducting transition temperature, T_c , even though Cooper pairs continue to survive up to a much higher temperature [5–8], T^* , giving rise to the so-called pseudogap state [9–13] between T_c and T^* . On the other hand, when a magnetic field is applied at low temperatures, one observes another intriguing phenomenon, the superconductor (S) to bad-metal/insulator (BM/I) transition [14–19]. At a characteristic magnetic field, H_c^* , the magnetoresistance isotherms intersect, giving rise to a state with negative temperature coefficient of resistance (R) above this field. In very strongly disordered superconductors such as InO_x and TiN this results in a strongly insulating state with diverging electrical resistance, sometimes called a superinsulator, which is believed to be the conjugate of the superconductor [20–22], where Cooper pairs instead of vortices are localized. On the other hand, when the disorder is more moderate, in several systems such as MoGe , Ta , and NbN , the resistance increases weakly with decreasing temperature and remains finite even as $T \rightarrow 0$; this state is more appropriately classified as a bad metal [15,23–27]. Whether Cooper pairs survive in this bad metal is an open question. Normally, a metallic state consisting of Cooper pairs is not expected since Cooper pairs are either in the eigenstate of the phase which gives a superconductor, or in the eigenstate of a number which gives an insulator. However, in recent years there have been suggestions that Cooper pairs could exist in a

dissipative state called a Bose metal [28–36] although its existence remains hotly debated [37–39]. Therefore, the metallic state above H_c^* in such systems deserves careful attention.

In this Letter, we investigate the field induced S-BM transition in a 2 nm thick amorphous $\text{Mo}_{70}\text{Ge}_{30}$ (*a*-MoGe) thin film, using a combination of low-temperature scanning tunneling spectroscopy (STS) and magnetotransport measurements. The primary advantage of STS is that it provides direct information on the local density of states. The central finding of this work is that the field induced bad-metal state shows spectroscopic characteristics that are consistent with the existence of phase incoherent Cooper pairs as predicted for a Bose metal.

II. METHODS

The *a*-MoGe film was grown by pulsed laser deposition. Details of sample growth and characterization have been reported elsewhere [40,41,13]. STS measurements were performed using a home-built low-temperature scanning tunneling microscope [42] (STM) operating down to 450 mK and up to a magnetic field of 90 kOe using a Pt-Ir normal metal tip. The tunneling conductance, $G(V) = \frac{dI}{dV}|_V$, as a function of voltage (V), was measured using the standard lock-in technique. To image vortices, spatially resolved $G(V)$ maps were recorded at a fixed voltage close to the coherence peak, where each vortex appears as a local minimum. We used an ultrahigh-vacuum suitcase to transport the sample after deposition and transfer in the STM without exposure to air. After completing STS measurements, the sample was transported back to the deposition chamber in the same way and covered with a 1 nm thick Si protective layer before transport measurements. Magnetotransport measurements were performed in a conventional ^3He cryostat. Since the magnetotransport properties of *a*-MoGe films are extremely susceptible to external electromagnetic radiation [43], all electrical feedthroughs

*pratap@tifr.res.in

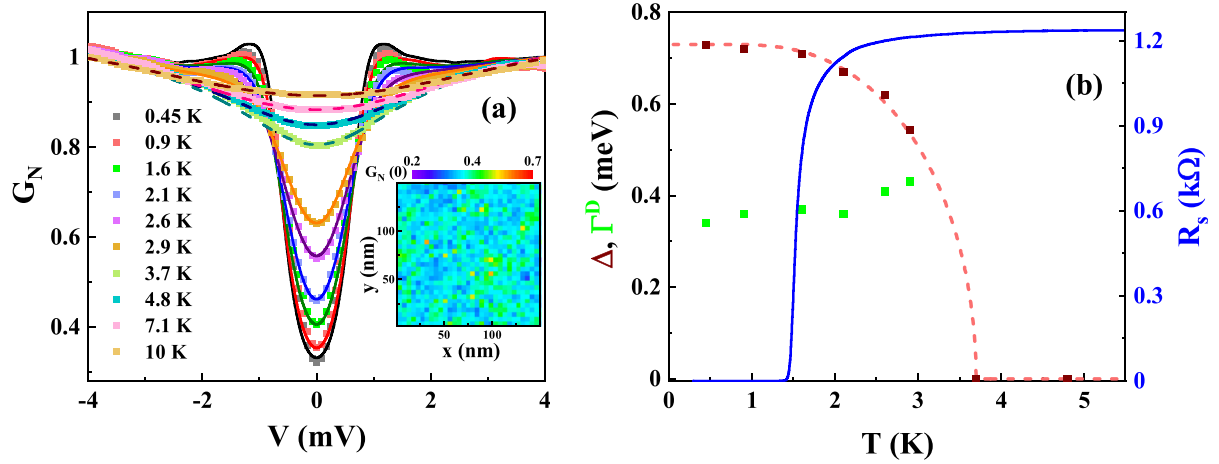


FIG. 1. (a) $G_N(V)$ - V tunneling spectra in zero field at different temperatures along with theoretical fit using Eq. (1). At 3.7 K and above the spectra are fitted with AA corrections alone (dashed line) whereas at lower temperatures additional contribution from superconductivity has to be incorporated (solid lines). Inset: Spatial map of $G_N(0)$ at 450 mK. (b) Temperature dependence of superconducting energy gap Δ and Γ^D (left axis) and sheet resistance R_s (right axis) at zero magnetic field; the dashed line is a guide to the eye that mimics the BCS temperature variation of Δ .

leading to the sample were fitted with RC filters with a very low cutoff frequency of 100 Hz.

III. RESULTS AND DISCUSSION

Figure 1(a) shows the normalized conductance, $G_N(V) = \frac{G(V)}{G(4 \text{ mV})}$, in zero field, averaged over a 32×32 grid over a $150 \text{ nm} \times 150 \text{ nm}$ area at various temperatures. Superconductivity manifests as a suppression of $G_N(V)$ for voltage, $|V| < \Delta/e$, and the appearance of coherence peaks at the gap edge. In disordered superconductors, we observe an additional V-shaped background that extends up to high bias [44–46], which originates from e - e Coulomb interactions described within Altshuler-Aronov (AA) theory [47–49]. In order to fit the data, incorporating both the AA correction and the effect of superconductivity, we adopt a procedure recently developed by Žemlička *et al.* [50]. At temperature T , the tunneling conductance is given in terms of the single particle density of states of the sample, $N(E)$, by the relation [51]

$$G(V, T) \propto \int_{-\infty}^{\infty} dE \frac{1}{k_B T} \frac{e^{\frac{E+eV}{k_B T}}}{\left(1 + e^{\frac{E+eV}{k_B T}}\right)^2} N(E), \quad (1)$$

where k_B is the Boltzmann constant. Here we assume the density of states of the Pt-Ir tip to be energy independent, which is a good approximation within tens of meV from the Fermi level. In a normal metal, AA corrections modify the bare density of states, N_N as [50]

$$N_N^{\text{AA}}(E) = N_N \left(1 + \tilde{\lambda}_0 [f_d(E, \Gamma_0) - \lambda_r [f_d(E, \Gamma_1) + f_d(E + E_z, \Gamma_1) + f_d(E - E_z, \Gamma_1)]]\right), \quad (2a)$$

$$f_d(E, \Gamma_n) = -\frac{1}{2} \int_0^{\frac{\Gamma_n}{k_B T}} dx \frac{x}{x^2 + \left(\frac{\Gamma_n}{k_B T}\right)^2} \frac{\sinh(x)}{\cosh(x) + \cosh\left(\frac{E}{k_B T}\right)}, \quad (2b)$$

where $\Gamma = \frac{\hbar}{\tau}$, τ is the transport scattering time, $E_z = 2\mu_B H$ (μ_B is the Bohr magneton) is the Zeeman energy when there

is an applied magnetic field H , and Γ_0 and Γ_1 account for the broadening due to energy and spin scattering. We use Γ_0 , Γ_1 , $\tilde{\lambda}_0$, and λ_r as adjustable parameters. In Fig. 1(a) we can fit the data for $T \geq 3.7 \text{ K}$ using Eq. (1), with $N(E) = N_N^{\text{AA}}(E)$; we take $E_z = 0$, $\Gamma_0 = \Gamma_1 = 0.2 \text{ meV}$. It is important to note that the parameters related to AA fitting do not vary more than $\pm 10\%$ from their mean value over the entire range of temperature and magnetic field which arises from statistical error. The complete set of best fit parameters is given in the Supplemental Material [52]. In principle, Γ is also a fitting parameter which we take as $\Gamma \sim 20 \text{ eV}$ based on $\tau \sim 3 \times 10^{-17} \text{ s}$ estimated from resistivity. However, for such a large value of Γ ($\gg \{k_B T, \Gamma_0, \Gamma_1\}$), Eq. (2b) is insensitive to its precise value and practically indistinguishable from setting the integration limit to infinity. For $T < 3.7 \text{ K}$, we cannot fit the data with AA contributions alone and need to incorporate the effect of superconductivity. In BCS theory where the density of state in the normal metal is assumed to be energy independent, the single particle density of states is given by [51] $N_s^{\text{BCS}}(E) = |\text{Re}\{\frac{E - i\Gamma^D}{\sqrt{(E - i\Gamma^D)^2 - \Delta^2}}\}|$, where Γ^D is a broadening parameter [53] that accounts for nonthermal sources of broadening. Even though Γ^D is introduced as a phenomenological parameter, this form is known to accurately reproduce the tunneling spectrum in a wide range of situations, both in the zero field and in the presence of magnetic field [50, 54–58]. When this correction is applied on top of the AA corrections, the single particle density of states is given by [50]

$$N(E) = N_s^{\text{BCS}}(E) N_N^{\text{AA}}(\Omega), \quad (3)$$

where $\Omega = \text{Re}\{\sqrt{(E - i\Gamma^D)^2 - \Delta^2}\}$; Ω in the second term ensures conservation in the number of states (and charge) above and below the superconducting transition. Using this form for $N(E)$ and Δ , Γ^D as fitting parameters, we can fit the $G_N(V)$ spectra down to 450 mK keeping Γ_0 and Γ_1 the same as the normal state value [Fig. 1(a)]. Figure 1(b) shows the

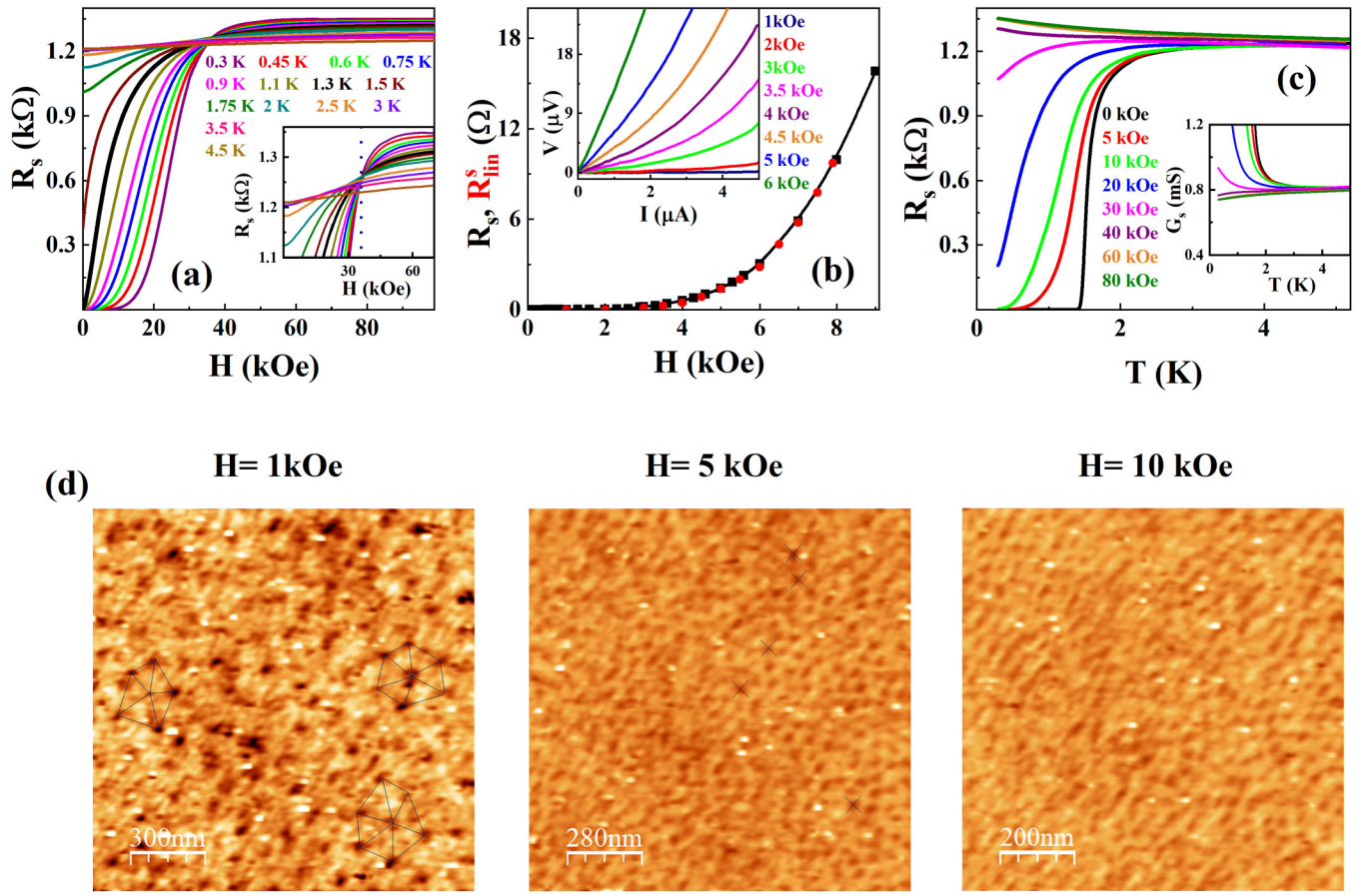


FIG. 2. (a) Magnetic field dependence of sheet resistance R_s at different temperatures. Inset: Expanded view of the same plot close to H_c^* (blue dotted line). (b) Plot of R_s (black square) and R_s^{lin} (red circle) vs H at low magnetic fields at 450 mK; inset: I - V characteristics at the same temperatures. (c) Temperature dependence of R_s at various magnetic fields. Inset shows corresponding temperature variation of sheet conductance G_s . (d) Spatial maps of $G_N(V)$ at the coherence peak voltage $V = 1.2$ mV at 450 mK for $H = 1, 5,$ and 10 kOe. At 1 kOe we observe a disordered vortex lattice; at 5 kOe individual vortices can be resolved only at some locations (such as the ones shown by \times) but in the rest of the area individual vortices cannot be identified; at 10 kOe we can no longer resolve individual vortices indicating that the vortex lattice has completely melted. Representative nearest neighbors are shown through connected black lines at a few representative locations for the image at 1 kOe.

temperature variation of Δ and Γ^D along with the temperature variation of the sheet resistance, R_s . $T_c \sim 1.36$ K is defined as the temperature where R_s is 0.05% of its normal state value. This temperature is much lower than $T^* \sim 3.7$ K where Δ vanishes, showing the existence of an extended pseudogap state. The zero bias conductance map at 450 mK [inset, Fig. 1(a)] shows large variations, forming puddlelike structures consistent with earlier reports [13].

We now turn our attention to the effect of magnetic field. Figure 2(a) shows R_s as a function of H . Below T_c , all the R_s - H curves cross close to $H_c^* \sim 36$ kOe which demarcates the S-BM transition [inset of Fig. 2(a)]. Concentrating first at low temperatures and low fields, we observe finite R_s above 3 kOe [Fig. 2(b)] at 450 mK. We confirm that this R_s indeed corresponds to the linear resistance, by plotting in the same graph $R_{\text{lin}} = \frac{dV}{dI}|_{I \rightarrow 0}$ calculated from current-voltage (I - V) characteristic measurements [inset of Fig. 2(b)]. At subcritical currents the resistance is dominated by thermally activated flux flow (TAFF) following the functional form, $R = R_{\text{ff}} \exp[-\frac{U(I)}{k_B T}]$, where R_{ff} is the Bardeen-Stephen flux flow resistance and $U(I)$ is the effective pinning barrier.

In a vortex solid the collective pinning barrier diverges with decreasing current, I , as $U(I) = U_0(\frac{I}{I_c})^\alpha$ ($\alpha \sim 1$) thereby giving a vanishing R_{lin} in the zero current limit [59,60]. In a vortex liquid (VL) $U(I)$ is independent of I and thus R_{lin} has finite value [61]. Further evidence of VL is obtained from STS images of the vortex state [Fig. 2(d)]. At 1 kOe we can resolve individual vortices even though the spatial configuration is extremely disordered; at 5 kOe some vortices are still visible but at many places we also observe blurred or elongated structures indicating considerable motion of vortices during the acquisition time of the image; at 10 kOe the vortex system is deep into VL and we cannot resolve individual vortices anymore. From R_s vs T at different H [Fig. 2(c)] we observe that for $H > H_c^*$, $\frac{dR_s}{dT} < 0$ down to 300 mK, even though the sheet conductance $G_s (= \frac{1}{R_s})$ extrapolates to a finite value as $T \rightarrow 0$, characteristic of a bad metal. Scaling analysis [62] of the R - H data close to H_c^* is given in the Supplemental Material [52].

To understand the evolution of the superconducting state at higher fields, we investigate the $G_N(V)$ vs V spectra, spatially averaged on a 32×32 grid over a $150 \text{ nm} \times 150 \text{ nm}$ area [Fig. 3(a)]. For $H > 70$ kOe the tunneling spectra can be fitted

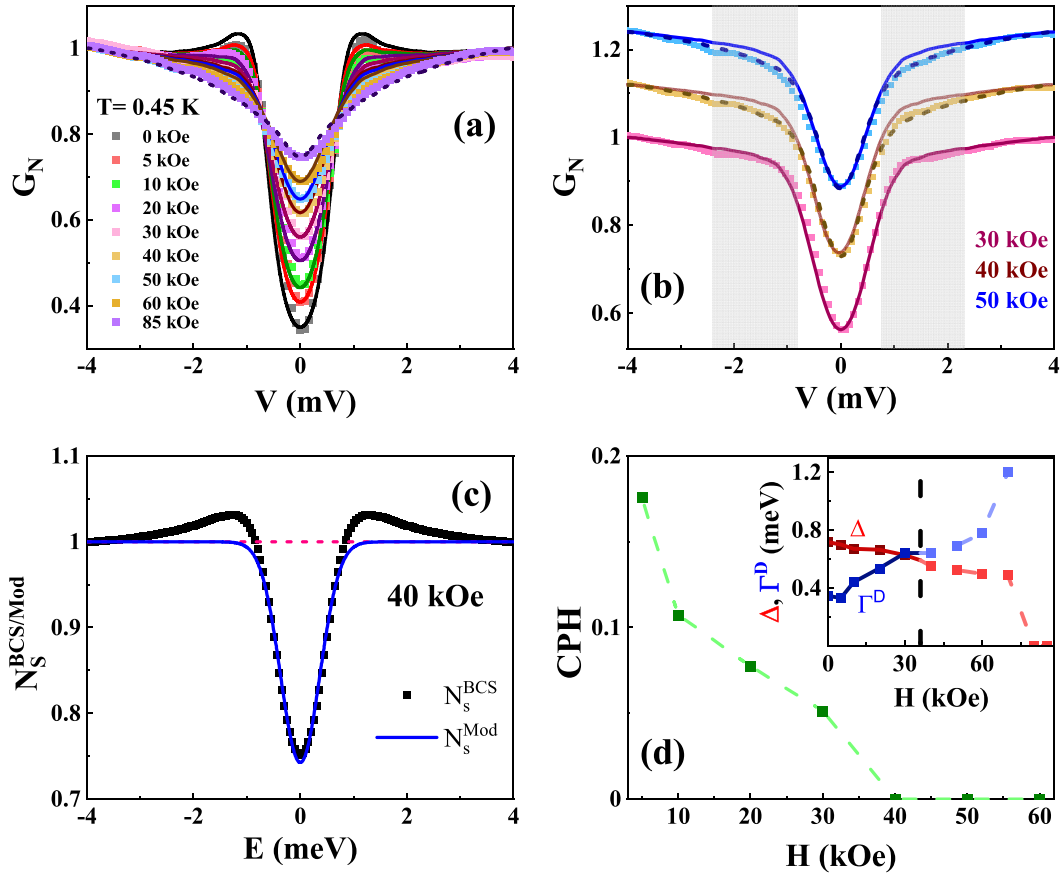


FIG. 3. (a) $G_N(V)$ vs V in different magnetic fields at 450 mK along with theoretical fit using Eq. (1). For $H > 70$ kOe the spectra are fitted with AA corrections alone (dashed line) whereas at lower temperatures additional contribution from superconductivity has to be incorporated (solid lines). (b) Fit of $G_N(V)$ vs V at $H = 30, 40,$ and 50 kOe using $N_s^{\text{BCS}}(E)$ (solid line) and $N_s^{\text{Mod}}(E)$ (dashed line) respectively; successive spectra following 30 kOe are shifted upward by 0.12 for clarity. For 40 and 50 kOe ($H > H_c^*$) the fit using $N_s^{\text{BCS}}(E)$ deviates significantly in the voltage range where the coherence peak appears (shaded gray region). (c) Plot of $N_s^{\text{BCS}}(E)$ (black dot) and $N_s^{\text{Mod}}(E)$ (blue solid line), used for the theoretical fit in (b) at 40 kOe. (d) Magnetic field dependence of coherence peak height (CPH). Inset: Variation of superconducting energy gap Δ , Γ^D as a function of magnetic field at 450 mK; for $H > H_c^*$, these values correspond to the values used in $N_s^{\text{BCS}}(E)$ from which $N_s^{\text{Mod}}(E)$ is constructed.

using $N(E) = N_N^{\text{AA}}(E)$. We define this field as H^* . Below H^* , we observe two distinct magnetic field regimes [Fig. 3(b)]. For $H < H_c^*$ we can fit the tunneling spectra using $N(E)$ in Eq. (3) with Δ and Γ^D as shown in the inset of Fig. 3(d). For $H^* \geq H > H_c^*$ this form is no longer adequate; we observe that the fitted value is larger in the voltage range corresponding to the energy where the coherence peaks are expected in $N_s^{\text{BCS}}(E)$. This deviation results from a complete suppression of the superconducting coherence peaks above H_c^* . To illustrate this point we modify $N_s^{\text{BCS}}(E)$ in the following way: We use the empirical form, $N_s^{\text{Mod}}(E) = \alpha_0 - A \exp(-BE^2)$, and adjust α_0 , A , and B such that $N_s^{\text{Mod}}(E) \approx N_s^{\text{BCS}}(E)$ when $N_s^{\text{Mod}}(E) \lesssim 0.95$, but asymptotically approaches 1 instead of exhibiting the coherence peak at higher values [Fig. 3(c)]. Using $N(E) = N_s^{\text{Mod}}(E)N_N^{\text{AA}}(\Omega)$ results in an excellent fit of the tunneling curves above H_c^* [Fig. 3(b)]. In Fig. 3(d), we plot the coherence peak height (CPH), defined as $\max\{N_s^{\text{BCS/Mod}}(E)\} - 1$. With increasing field CPH gradually reduces and becomes zero above H_c^* .

To understand the physical implication of these results we note that, while the superconducting energy gap is a direct manifestation of the pairing of electrons forming Cooper

pairs, the superconducting state requires another ingredient, namely, the global phase coherence among Cooper pairs, which is related to the appearance of the coherence peaks at the gap edge [51]. If Cooper pairs lack phase coherence, it is expected that the single particle spectrum will remain gapped, but the coherence peaks will get suppressed [2,4,7,63]. In a magnetic field, the nucleation of vortices complicates this scenario. Here both the gap and the coherence peaks vanish inside the vortex core but appear as one goes further from the vortex center. In a VL, where vortices are rapidly moving, a slow measurement such as STS measures the time averaged tunneling spectrum which has contributions from both inside and outside the core. This broadens the spectrum by partially filling the gap and suppressing the coherence peaks. It has been shown [55] that the average spectrum in the mixed state can be captured by adjusting Γ^D . This accounts for the gradual increase in Γ^D and suppression of CPH below H_c^* . On the other hand, the abrupt disappearance of the CPH for $H^* \geq H > H_c^*$, with no commensurate filling of the gap indicates that the Cooper pairs no longer have phase coherence. In conjunction with G_s in the $T \rightarrow 0$ limit, this implies the formation of a dissipative state made of Cooper pairs, i.e., a

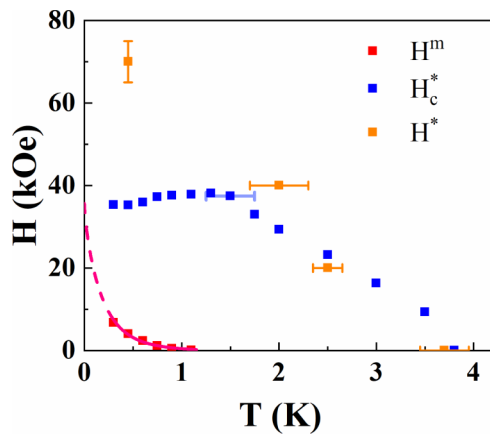


FIG. 4. Phase diagram showing the temperature evolution of H^* (orange square), H_c^* (blue square), and H^m (red square); the dashed line is the fit to the thermal melting line. The Bose metal phase is realized between H_c^* and H^* . In between H^m and H_c^* we have a vortex liquid.

Bose metal. We would like to note that this state is distinct from the zero field pseudogap state, where, as shown before, the spatially averaged spectra do not undergo any qualitative change across T_c . The origin of the pseudogap state lies in the emergence of tens of nanometer-sized superconducting puddles [64,65] separated by insulating regions and thermal fluctuations between these puddles that destroy the zero resistance state [13,66]. Here, even though we observe inhomogeneity in $G_N(0)$, the complete suppression of CPH in the average spectrum suggests that the coherence peak is uniformly suppressed everywhere. This has been further confirmed [52] by selectively fitting spectra in regions of high and low $G_N(0)$.

In Fig. 4 we show the phase boundaries of H_c^* and H^* in the H - T parameter space. The H^* boundary is determined from STS measurement and is defined as the highest magnetic field (at fixed temperature) or highest temperature (at fixed field) where the tunneling spectra cannot be fitted with the AA contribution alone [52]. The H_c^* boundary, on the other hand, is defined from the magnetic field at which two magnetoresistance curves at successive temperatures intersect. As expected for a quantum phase transition, this boundary is nearly temperature independent until about T_c ; above T_c it closely

follows the H^* boundary. Finally, we define the vortex lattice melting boundary, H^m , above which a finite linear resistance appears. The temperature variation of H^m is described very well by the formula for thermal melting [60,52] of the vortex lattice if one substitutes H_c^* for the upper critical field.

To place things into perspective all our results lead to the conclusion that above and below H_c^* there exist two distinct dissipative states demarcated by distinct transport and spectroscopic signatures. While the state below H_c^* is a classical VL, the question remains as to what the other state which we phenomenologically classify as a Bose metal is. Though we cannot conclusively settle this question here, one possibility is that it is a quantum VL. In a recent paper [67], it was shown that vortices in a 20 nm thick a -MoGe film undergo quantum zero-point fluctuations, whose fractional amplitude with respect to intervortex separation increases with increasing magnetic field. Here, a similar analysis shows [52] that the zero-point fluctuation amplitude of the vortices is expected to be about half the intervortex separation at H_c^* , such that quantum tunneling could be the dominant mechanism of vortex motion above this field. Whether such a state would display the complete suppression of the coherence peak needs to be theoretically investigated. The other point to note is that in our experiment the Bose metal exists only for $T \lesssim T_c$, when the zero field state can sustain a finite supercurrent, even though fragmented superconducting puddles continue to exist up to T^* .

IV. CONCLUSION

In summary, we have shown spectroscopic signatures that are consistent with the existence of a magnetic field induced Bose metal in an ultrathin a -MoGe thin film. In the future, it would be interesting to obtain a more direct proof of pairing from the charge of the carrier through measurements such as shot noise [68]. These results have relevance to other systems such as high-temperature superconductors [31] where Bose metal states have been reported. We hope that our results will bolster further theoretical investigations on how such a state emerges in a two-dimensional superconductor.

ACKNOWLEDGMENTS

We thank Nandini Trivedi for valuable suggestions. This paper was supported by the Department of Atomic Energy, Government of India (Grant No. 12-R&D-TFR-5.10-0100).

- [1] A. Ghosal, M. Randeria, and N. Trivedi, Role of Spatial Amplitude Fluctuations in Highly Disordered s -Wave Superconductors, *Phys. Rev. Lett.* **81**, 3940 (1998).
- [2] M. V. Feigel'man, L. B. Ioffe, V. E. Kravtsov, and E. A. Yuzbashyan, Eigenfunction Fractality and Pseudogap State Near the Superconductor-Insulator Transition, *Phys. Rev. Lett.* **98**, 027001 (2007).
- [3] Y. Dubi, Y. Meir, and Y. Avishai, Nature of the superconductor-insulator transition in disordered superconductors, *Nature (London)* **449**, 876 (2007).
- [4] M. V. Feigel'man, L. B. Ioffe, V. E. Kravtsov, and E. Cuevas, Fractal superconductivity near localization threshold, *Ann. Phys.* **325**, 1390 (2010).
- [5] V. J. Emery and S. A. Kivelson, Importance of phase fluctuations in superconductors with small superfluid density, *Nature (London)* **374**, 434 (1995).
- [6] A. Ghosal, M. Randeria, and N. Trivedi, Inhomogeneous pairing in highly disordered s -wave superconductors, *Phys. Rev. B* **65**, 014501 (2001).
- [7] K. Bouadim, Y. L. Loh, M. Randeria, and N. Trivedi, Single- and two-particle energy gaps across the disorder-driven superconductor-insulator transition, *Nat. Phys.* **7**, 884 (2011).
- [8] P. Raychaudhuri and S. Dutta, Phase fluctuations in conventional superconductors, *J. Phys.: Condens. Matter* **34**, 083001 (2022).

- [9] B. Sacépé, C. Chapelier, T. I. Baturina, V. M. Vinokur, M. R. Baklanov, and M. Sanquer, Pseudogap in a thin film of a conventional superconductor, *Nat. Commun.* **1**, 140 (2010).
- [10] M. Mondal, A. Kamlapure, M. Chand, G. Saraswat, S. Kumar, J. Jesudasan, L. Benfatto, V. Tripathi, and P. Raychaudhuri, Phase Fluctuations in a Strongly Disordered s -Wave NbN Superconductor Close to the Metal-Insulator Transition, *Phys. Rev. Lett.* **106**, 047001 (2011).
- [11] B. Sacepe, T. Dubouchet, C. Chapelier, M. Sanquer, M. Ovidia, D. Shahar, M. Feigel'man, and L. Ioffe, Localization of preformed Cooper pairs in disordered superconductors, *Nat. Phys.* **7**, 239 (2011).
- [12] T. Dubouchet, B. Sacépé, J. Seidemann, D. Shahar, M. Sanquer, and C. Chapelier, Collective energy gap of preformed Cooper pairs in disordered superconductors, *Nat. Phys.* **15**, 233 (2019).
- [13] S. Mandal, S. Dutta, S. Basistha, I. Roy, J. Jesudasan, V. Bagwe, L. Benfatto, A. Thamizhavel, and P. Raychaudhuri, Destruction of superconductivity through phase fluctuations in ultrathin a -MoGe films, *Phys. Rev. B* **102**, 060501(R) (2020).
- [14] A. F. Hebard and M. A. Paalanen, Magnetic-Field-Tuned Superconductor-Insulator Transition in Two-Dimensional Films, *Phys. Rev. Lett.* **65**, 927 (1990).
- [15] A. Yazdani and A. Kapitulnik, Superconducting-Insulating Transition in Two-Dimensional a -MoGe Thin Films, *Phys. Rev. Lett.* **74**, 3037 (1995).
- [16] E. Bielejec and W. Wu, Field-Tuned Superconductor-Insulator Transition with and without Current Bias, *Phys. Rev. Lett.* **88**, 206802 (2002).
- [17] V. F. Gantmakher, M. V. Golubkov, V. T. Dolgoplov, A. A. Shashkin, and G. E. Tsydynzhapov, Observation of the parallel-magnetic-field-induced superconductor-insulator transition in thin amorphous InO Films, *JETP Lett.* **71**, 160 (2000).
- [18] G. Sambandamurthy, L. W. Engel, A. Johansson, and D. Shahar, Superconductivity-Related Insulating Behavior, *Phys. Rev. Lett.* **92**, 107005 (2004).
- [19] T. I. Baturina, D. R. Islamov, J. Bentner, C. Strunk, M. R. Baklanov, and A. Satta, Superconductivity on the localization threshold and magnetic-field-tuned superconductor-insulator transition in TiN films, *JETP Lett.* **79**, 337 (2004).
- [20] V. M. Vinokur, T. I. Baturina, M. V. Fistul, A. Yu. Mironov, M. R. Baklanov, and C. Strunk, Superinsulator and quantum synchronization, *Nature (London)* **452**, 613 (2008).
- [21] M. Ovidia, D. Kalok, B. Sacépé, and D. Shahar, Duality symmetry and its breakdown in the vicinity of the superconductor-insulator transition, *Nat. Phys.* **9**, 415 (2013).
- [22] S. Sankar, V. M. Vinokur, and V. Tripathi, Disordered Berezinskii-Kosterlitz-Thouless transition and superinsulation, *Phys. Rev. B* **97**, 020507(R) (2018).
- [23] N. Mason and A. Kapitulnik, Dissipation Effects on the Superconductor-Insulator Transition in 2D Superconductors, *Phys. Rev. Lett.* **82**, 5341 (1999).
- [24] M. Chand, G. Saraswat, A. Kamlapure, M. Mondal, S. Kumar, J. Jesudasan, V. Bagwe, L. Benfatto, V. Tripathi, and P. Raychaudhuri, Phase diagram of the strongly disordered s -wave superconductor NbN close to the metal-insulator transition, *Phys. Rev. B* **85**, 014508 (2012).
- [25] Y. Qin, C. L. Vicente, and J. Yoon, Magnetically induced metallic phase in superconducting tantalum films, *Phys. Rev. B* **73**, 100505(R) (2006).
- [26] I. Zaytseva, A. Abaloszew, B. C. Camargo, Y. Syryanyy, and M. Z. Cieplak, Upper critical field and superconductor-metal transition in ultrathin niobium films, *Sci. Rep.* **10**, 19062 (2020).
- [27] W. Liu, L. Pan, J. Wen, M. Kim, G. Sambandamurthy, and N. P. Armitage, Microwave Spectroscopy Evidence of Superconducting Pairing in the Magnetic-Field-Induced Metallic State of InO_x Films at Zero Temperature, *Phys. Rev. Lett.* **111**, 067003 (2013).
- [28] P. Phillips and D. Dalidovich, The elusive Bose metal, *Science* **302**, 243 (2003).
- [29] J. Wu and P. Phillips, Vortex glass is a metal: Unified theory of the magnetic-field and disorder-tuned Bose metals, *Phys. Rev. B* **73**, 214507 (2006).
- [30] B. Spivak, P. Oredo, and S. A. Kivelson, Theory of quantum metal to superconductor transitions in highly conducting systems, *Phys. Rev. B* **77**, 214523 (2008).
- [31] C. Yang, Y. Liu, Y. Wang, L. Feng, Q. He, J. Sun, Y. Tang, C. Wu, J. Xiong, W. Zhang, X. Lin, H. Yao, H. Liu, G. Fernandez, J. Xu, J. M. Valles, Jr., J. Wang, and Y. Li, Intermediate bosonic metallic state in the superconductor-insulator transition, *Science* **366**, 1505 (2019).
- [32] T. Ren and A. M. Tsvelik, How magnetic field can transform a superconductor into a Bose metal, *New J. Phys.* **22**, 103021 (2020).
- [33] P. Phillips and D. Dalidovich, Short-range interactions and a Bose metal phase in two dimensions, *Phys. Rev. B* **65**, 081101(R) (2002).
- [34] S. Doniach and D. Das, The Bose metal—a commentary, *Braz. J. Phys.* **33**, 740 (2003).
- [35] M. C. Diamantini, A. Yu. Mironov, S. M. Postolova, X. Liu, Z. Hao, D. M. Silevitch, Ya. Kopelevich, P. Kim, C. A. Trugenberger, and V. M. Vinokur, Bosonic topological insulator intermediate state in the superconductor-insulator transition, *Phys. Lett. A* **384**, 126570 (2020).
- [36] D. Das and S. Doniach, Bose metal: Gauge-field fluctuations and scaling for field-tuned quantum phase transitions, *Phys. Rev. B* **64**, 134511 (2001).
- [37] I. Tamir, A. Benyamini, E. J. Telford, F. Gorniaczyk, A. Doron, T. Levinson, D. Wang, F. Gay, B. Sacépé, J. Hone, K. Watanabe, T. Taniguchi, C. R. Dean, A. N. Pasupathy, and D. Shahar, Sensitivity of the superconducting state in thin films, *Sci. Adv.* **5**, eaau3826 (2019).
- [38] P. W. Phillips, Free at last: Bose metal uncaged, *Science* **366**, 1450 (2019).
- [39] X. Zhang, B. Hen, A. Palevski, and A. Kapitulnik, Robust anomalous metallic states and vestiges of self-duality in two-dimensional granular In-InO_x composites, *npj Quantum Mater.* **6**, 30 (2021).
- [40] I. Roy, S. Dutta, A. N. Roy Choudhury, S. Basistha, I. Maccari, S. Mandal, J. Jesudasan, V. Bagwe, C. Castellani, L. Benfatto, and P. Raychaudhuri, Melting of the Vortex Lattice through Intermediate Hexatic Fluid in an a -MoGe Thin Film, *Phys. Rev. Lett.* **122**, 047001 (2019).
- [41] S. Dutta, I. Roy, S. Basistha, S. Mandal, J. Jesudasan, V. Bagwe, and P. Raychaudhuri, Collective flux pinning in hexatic vortex fluid in a -MoGe thin film, *J. Phys.: Condens. Matter* **32**, 075601 (2020).
- [42] A. Kamlapure, G. Saraswat, S. C. Ganguli, V. Bagwe, P. Raychaudhuri, and S. P. Pai, A 350 mK, 9 T scanning tunneling microscope for the study of superconducting thin films on

- insulating substrates and single crystals, *Rev. Sci. Instrum.* **84**, 123905 (2013).
- [43] S. Dutta, I. Roy, S. Mandal, J. Jesudasan, V. Bagwe, and P. Raychaudhuri, Extreme sensitivity of the vortex state in a -MoGe films to radio-frequency electromagnetic perturbation, *Phys. Rev. B* **100**, 214518 (2019).
- [44] S. P. Chockalingam, M. Chand, A. Kamlapure, J. Jesudasan, A. Mishra, V. Tripathi, and P. Raychaudhuri, Tunneling studies in a homogeneously disordered s -wave superconductor: NbN, *Phys. Rev. B* **79**, 094509 (2009).
- [45] C. Carbillet, V. Cherkov, M. A. Skvortsov, M. V. Feigel'man, F. Debontridder, L. B. Ioffe, V. S. Stolyarov, K. Ilin, M. Siegel, D. Roditchev, T. Cren, and C. Brun, Spectroscopic evidence for strong correlations between local resistance and superconducting gap in ultrathin NbN films, *Phys. Rev. B* **102**, 024504 (2020).
- [46] S. V. Postolova, A. Yu. Mironov, V. Barrena, J. Benito-Llorens, J. G. Rodrigo, H. Suderow, M. R. Baklanov, T. I. Baturina, and V. M. Vinokur, Superconductivity in a disordered metal with Coulomb interactions, *Phys. Rev. Res.* **2**, 033307 (2020).
- [47] B. L. Altshuler and A. G. Aronov, in *Electron-Electron Interactions in Disordered Systems*, Modern Problems in Condensed Matter Sciences, edited by A. Efros and M. Pollak (Elsevier, Amsterdam, 1985), pp. 1–153.
- [48] B. L. Altshuler, A. G. Aronov, and P. A. Lee, Interaction Effects in Disordered Fermi Systems in Two Dimensions, *Phys. Rev. Lett.* **44**, 1288 (1980).
- [49] B. L. Altshuler and A. G. Aronov, Zero bias anomaly in tunnel resistance and electron-electron interaction, *Solid State Commun.* **30**, 115 (1979).
- [50] M. Žemlička, M. Kopčík, P. Szabó, T. Samuely, J. Kačmarčík, P. Neilinger, M. Grajcar, and P. Samuely, Zeeman-driven superconductor-insulator transition in strongly disordered MoC films: Scanning tunneling microscopy and transport studies in a transverse magnetic field, *Phys. Rev. B* **102**, 180508(R) (2020).
- [51] M. Tinkham, *Introduction to Superconductivity* (McGraw-Hill, New York, 1996).
- [52] See Supplemental Material at <http://link.aps.org/supplemental/10.1103/PhysRevB.105.L140503> for (i) fit of the spectra at 450 mK, 40 kOe and regions of high and low $G_N(0)$; (ii) fit of the H^m line in the H - T parameter space with the theory of thermal vortex melting; (iii) the complete table of best fit parameters for the tunneling spectra; (iv) analysis of possible zero-point fluctuation of vortices; (v) scaling analysis of the magnetoresistance curves; and (vi) determination of H^* in H - T parameter space.
- [53] R. C. Dynes, V. Narayanamurti, and J. P. Garno, Direct Measurement of Quasiparticle-Lifetime Broadening in a Strongly-Coupled Superconductor, *Phys. Rev. Lett.* **41**, 1509 (1978).
- [54] R. S. Gonnelli, D. Daghero, A. Calzolari, G. A. Ummarino, V. Dellarocca, V. A. Stepanov, J. Jun, S. M. Kazakov, and J. Karpinski, Magnetic-field dependence of the gaps in a two-band superconductor: A point-contact study of MgB₂ single crystals, *Phys. Rev. B* **69**, 100504(R) (2004).
- [55] S. Mukhopadhyay, G. Sheet, P. Raychaudhuri, and H. Takeya, Magnetic-field dependence of superconducting energy gaps in YNi₂B₂C: Evidence of multiband superconductivity, *Phys. Rev. B* **72**, 014545 (2005).
- [56] T. Le, L. Yin, Z. Feng, Q. Huang, L. Che, J. Li, Y. Shi, and X. Lu, Single full gap with mixed type-I and type-II superconductivity on surface of the type-II Dirac semimetal PdTe₂ by point-contact spectroscopy, *Phys. Rev. B* **99**, 180504(R) (2019).
- [57] A. Sirohi, S. Saha, P. Neha, S. Das, S. Patnaik, T. Das, and G. Sheet, Multiband superconductivity in Mo₈Ga₄₁ driven by a site-selective mechanism, *Phys. Rev. B* **99**, 054503 (2019).
- [58] F. Herman and R. Hlubina, Microscopic interpretation of the Dynes formula for the tunneling density of states, *Phys. Rev. B* **94**, 144508 (2016).
- [59] M. V. Feigel'man, V. B. Geshkenbein, A. I. Larkin, and V. M. Vinokur, Theory of Collective Flux Creep, *Phys. Rev. Lett.* **63**, 2303 (1989).
- [60] G. Blatter, M. V. Feigel'man, V. B. Geshkenbein, A. I. Larkin, and V. M. Vinokur, Vortices in high-temperature superconductors, *Rev. Mod. Phys.* **66**, 1125 (1994).
- [61] V. M. Vinokur, M. V. Feigel'man, V. B. Geshkenbein, and A. I. Larkin, Resistivity of High- T_c Superconductors in a Vortex-Liquid State, *Phys. Rev. Lett.* **65**, 259 (1990).
- [62] M. P. A. Fisher, Quantum Phase Transitions in Disordered Two-Dimensional Superconductors, *Phys. Rev. Lett.* **65**, 923 (1990).
- [63] G. Lemarie, A. Kamlapure, D. Bucheli, L. Benfatto, J. Lorenzana, G. Seibold, S. C. Ganguli, P. Raychaudhuri, and C. Castellani, Universal scaling of the order-parameter distribution in strongly disordered superconductors, *Phys. Rev. B* **87**, 184509 (2013).
- [64] B. Sacépé, C. Chapelier, T. I. Baturina, V. M. Vinokur, M. R. Baklanov, and M. Sanquer, Disorder-Induced Inhomogeneities of the Superconducting State Close to the Superconductor-Insulator Transition, *Phys. Rev. Lett.* **101**, 157006 (2008).
- [65] A. Kamlapure, T. Das, S. C. Ganguli, J. B. Parmar, S. Bhattacharyya, and P. Raychaudhuri, Emergence of nanoscale inhomogeneity in the superconducting state of a homogeneously disordered conventional superconductor, *Sci. Rep.* **3**, 2979 (2013).
- [66] M. Mondal, A. Kamlapure, S. C. Ganguli, J. Jesudasan, V. Bagwe, L. Benfatto, and P. Raychaudhuri, Enhancement of the finite-frequency superfluid response in the pseudogap regime of strongly disordered superconducting films, *Sci. Rep.* **3**, 1357 (2013).
- [67] S. Dutta, I. Roy, J. Jesudasan, S. Sachdev, and P. Raychaudhuri, Evidence of zero-point fluctuation of vortices in a very weakly pinned a -MoGe thin film, *Phys. Rev. B* **103**, 214512 (2021).
- [68] K. M. Bastiaans, D. Chatzopoulos, J.-F. Ge, D. Cho, W. O. Tromp, J. M. van Ruitenbeek, M. H. Fischer, P. J. de Visser, D. J. Thoen, E. F. C. Driessen, T. M. Klapwijk, and M. P. Allan, Direct evidence for Cooper pairing without a spectral gap in a disordered superconductor above T_c , *Science* **374**, 608 (2021).

Correction: The previously published Figure 2(b) contained an error in the x-axis label and has been replaced.